

NASA Technical Memorandum 105969

1N-02
137551
P-14

An Overview of Shed Ice Impact Studies in the NASA Lewis Icing Research Tunnel

Randall K. Britton
Sverdrup Technology Inc.
Brook Park, Ohio

and

Thomas H. Bond
Lewis Research Center
Cleveland, Ohio

Prepared for the
31st Aerospace Sciences Meeting
sponsored by the American Institute of Aeronautics and Astronautics
Reno, Nevada, January 11-14, 1993

(NASA-TM-105969) AN OVERVIEW OF
SHED ICE IMPACT IN THE NASA LEWIS
ICING RESEARCH TUNNEL (NASA) 14 p

N93-15404

Unclass

NASA

G3/02 0137551



An Overview of Shed Ice Impact Studies In The NASA Lewis Icing Research Tunnel

Randall K. Britton
Sverdrup Technology, Inc.
NASA Lewis Research Center Group
Brook Park, Ohio

Thomas H. Bond
NASA Lewis Research Center
Cleveland, Ohio

ABSTRACT

One of the areas of active research in commercial and military rotorcraft is directed toward developing the capability of sustained flight in icing conditions. The emphasis to date has been on the accretion and subsequent shedding of ice in an icing environment, where the shedding may be natural or induced. Historically, shed-ice particles have been a problem for aircraft, particularly rotorcraft. Because of the high particle velocities involved, damage to a fuselage or other airframe component from a shed-ice impact can be significant. Design rules for damage tolerance from shed-ice impact are not well developed because of a lack of experimental data. Thus, the NASA Lewis Research Center (LeRC) has begun an effort to develop a database of impact force and energy resulting from shed ice. This effort consisted of a test of NASA LeRC's Model Rotor Test Rig (MRTR) in the Icing Research Tunnel (IRT). Both natural shedding and forced shedding were investigated. Forced shedding was achieved by fitting the rotor blades with Small Tube Pneumatic (STP) de-icer boots manufactured by BF Goodrich. A detailed description of the test is given as well as the design of a new impact sensor which measures the force-time history of an impacting ice fragment. A brief discussion of the procedure to infer impact energy from a force-time trace is also included. Extensive high-speed imaging was used to measure shed-ice particle size, velocity, and trajectory. These quantities, in conjunction with the force-time trace are required for the impact-energy

calculations. Recommendations and future plans for this research area are also provided.

NOMENCLATURE

E_o	Initial kinetic energy
ΔE	Absorbed energy
F	Applied force
m	Particle mass
Δp	Change in momentum
v_o	Initial velocity
v_f	Final velocity

INTRODUCTION

An icing analysis of a rotating system differs from that of a fixed system in that shedding becomes a predominant factor.¹ This is because shedding controls the radial extent of ice on the rotor/propeller. The radial extent of ice directly affects the amount of power required to maintain flight. For the specific case of a helicopter main rotor, the combination of centrifugal force and vibratory airloads make ice shedding commonplace. In a general sense, natural ice shedding occurs when the centrifugal, bending, vibratory, and aerodynamic forces acting on a mass of ice overcome the ice adhesion forces that bond the ice to the surface. Rotorcraft manufacturers have to be concerned with what happens to the ice leaving the rotating blade. They need to know what force/energy the shed ice is capable of delivering to a surface such as the fuselage, a trailing rotor blade, etc. in the event of an impact.

The Icing Branch at NASA Lewis Research Center (LeRC) surveyed the four major U.S. helicopter manufacturers to determine what type of information would be most helpful to obtain from a model rotor test in the Icing Research Tunnel (IRT). The specified industry needs were as follows:

- 1) Time history of shedding during an icing encounter
- 2) Radial location of shedding during an icing encounter
- 3) Shed ice size and history of ice particle break-up
- 4) Shed ice trajectory
- 5) Impact energy of shed ice particles against a known material

Because of the development of a new force-sensing technology and recent improvements in high-speed imaging capability at LeRC, it was felt that all 5 points above could be documented. However, measurement of the shed-ice particle impact energy has been given priority in this project. The high-speed imaging is used to record shed-ice particle size, velocity, and trajectory. This information, along with the impact force recorded from a NASA-designed sensor plate can be used to infer impact energy.

Measuring the energy absorbed by a component due to an ice impact is rather difficult in that the impact is not elastic. Were the impact elastic the procedure would be to measure the velocity of the particle before and after the collision. Then, if the mass of the particle is known the energy absorbed by the wall would be:

$$\Delta E = \frac{1}{2}mv_o^2 - \frac{1}{2}mv_f^2 \quad (1)$$

assuming no rotation in the body. This is illustrated in Figure 1. Unfortunately, when an ice particle strikes a component it usually fractures into many particles - so many that it is virtually impossible to measure the size and velocity of each one (Figure 2). So for this

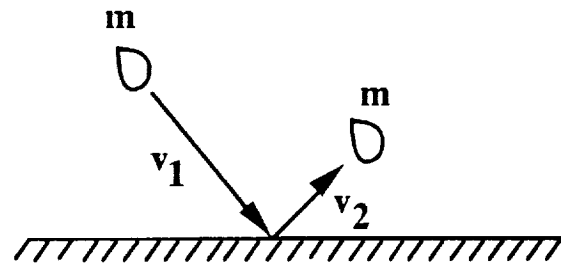


Figure 1. Perfectly elastic collision.

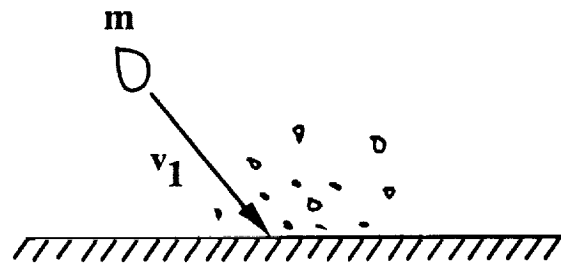


Figure 2. Shed ice particle collision.

application, the energy absorbed must be determined without the use of any information after the impact. Equation (1) which defines absorbed energy can be manipulated to look like:

$$\Delta E = mv_o^2 - mv_ov_f - \frac{1}{2}mv_o^2 + mv_ov_f - \frac{1}{2}mv_f^2 \quad (2)$$

Grouping the last three terms,

$$\Delta E = mv_o^2 - mv_ov_f - \frac{(mv_o^2 - mv_ov_f)^2}{2mv_o^2} \quad (3)$$

Now, the term:

$$mv_o^2 - mv_ov_f$$

can be rewritten as:

$$v_o m(v_o - v_f)$$

which is really the incoming velocity times the

change in momentum of the particle before and after the impact. The change in momentum of a particle can be expressed as:

$$\Delta p = \int_0^t F dt = m(v_o - v_f) \quad (4)$$

Therefore, it is possible to define a term, E_A as:

$$E_A = v_o m(v_o - v_f) = v_o \Delta p \quad (5)$$

so that the expression for the energy absorbed by the wall becomes:

$$\Delta E = E_A - \frac{E_A^2}{4E_o} \quad (6)$$

where E_o is the ice particle's incoming kinetic energy. Imaging techniques permit the determination of the particle's incoming velocity, v_o and mass, m . A record of the impact force as a function of time permits the calculation of the impulse, Δp . Thus, the energy absorbed by the wall due to particle impact can be calculated from equation (6). To implement this procedure, it was necessary to develop a sensor to record the impact force as a function of time.

During the sensor system development it became clear that the technique used to record the force-time traces of shed ice particle impacts would require a significant amount of proof of concept testing under controlled conditions. Thus, a two-phase approach was selected. Phase I proof-of-concept testing was performed at the University of Toledo ice gun facility. Here, conditions such as the ice particle mass and velocity were easily controlled. The Impact Energy Measurement System (IEMS) developed at the University of Toledo ice gun facility was tested in the IRT in Phase II as part of the shed ice impact study. During this study, it was desired to obtain data from natural shedding events. However, natural ice shedding from a rotating system is a very unpredictable phenomena. To overcome this obstacle, a deicing system was used. The

blades were fitted with Small Tube Pneumatic (STP) deicing boots, provided by BFGoodrich De-Icing Systems. This allowed for triggering the shed event and high speed cameras at a specified time. A complete description of the STP system is given in a later section.

The IRT entry lasted from May 4 through June 5, 1992. A total of over 300 ice impact events with peak impact forces ranging from 0.5 to 200 lbs were recorded over 16 days of actual testing. Although the majority of data was taken with the STP system installed, some of the data includes natural shedding events. This paper will provide a description of the testing procedure as well as a sample of the data taken. A detailed discussion of the results will be provided at a later time after data reduction and analysis has been completed.

TEST APPARATUS DESCRIPTION

Icing Research Tunnel

The IRT is a closed-loop refrigerated wind tunnel. A 5000 HP fan provides airspeeds up to 134 m/sec (300 mph). The heat exchanger can control the total temperature in the test section from -1.1 to -42 °C. The spray nozzles provide droplet sizes from approximately 10 to 40 μ m median volume droplet (MVD) diameter with liquid water contents (LWC) ranging from 0.2 to 3.0 g/m³. The test section of the tunnel is 1.83 m (6 ft) high and 2.74 m (9 ft) wide.

In the event of an asymmetric ice shedding event, vibration levels can be excessive on the model rotor test rig. These extremely high vibration levels cause a higher likelihood of catastrophic failure of the rotating hardware. Thus, the tunnel test section walls, which have an array of visual access windows were covered with 1" thick armor plating to protect personnel from any potential danger. Video systems were installed to monitor the test section and model.

Model Rotor Test Rig (MRTR)

The MRTR was composed of the tail shaft, hub, teetering components, and rotor blades from an OH-58 helicopter (Figure 3

(C-92-4100)). The rotor blades were NACA

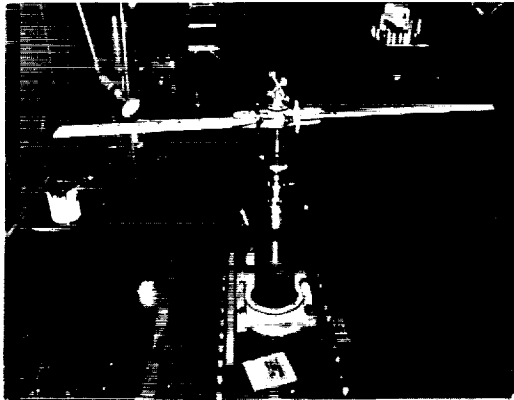


Figure 3. NASA LeRC Model Rotor Test Rig (MRTR).

0012 airfoils with a chord of 0.133 m (5.25 in) and a span of 0.73 m (28.74 in). The total diameter of the rotor assembly was 1.575 m (5.17 ft). This assembly was mated, through an adapter, to a 2.1 m (6.89 ft) long drive shaft. The extended drive shaft allowed the rotor blades to be run in the horizontal plane in the middle of the test section of the IRT while the drive system hardware remained below the tunnel turntable (Figure 4 (C-92-4095)). There was a hydraulically operated center tube which controlled the collective pitch of the rotor blades. This provided the ability to change blade angle quickly to the desired condition. The drive housing was bolted to the tunnel floor plate via two gimbal pins. An adjustable locking mechanism allowed the rotor assembly to be tilted in the fore and aft plane. For this test the rotor shaft was set at 5° forward tilt to simulate forward flight of a helicopter.

The drive shaft was connected to a 100 HP DC electric motor by a 3 belt pulley system. The motor was controlled by a SCR adjustable speed drive. This drive assembly was chosen because of its flexibility to handle the variable torque loads.

The MRTR was instrumented to provide data collection and safety monitoring capabilities. The critical safety items were rig vibration, bearing temperatures, percent drive

speed, and torque. There were four accelerometers and four thermocouples mounted on the drive system. The thermocouples monitored the bearing temperatures. The accelerometers provided information about radial and thrust vibration on the upper bearing and radial vibration on the lower bearing. The output was converted to velocity at the charge amplifiers. This provided vibration output for the rotating system that could be easily compared to known levels of concern from standard rotating equipment out-of-balance nomographs. A speed pick-up was mounted on the DC motor shaft. This allowed comparison to the drive shaft speed to monitor belt slippage. The hydraulic system pressure and fluid reservoir were monitored to assure the operability of the collective pitch system.

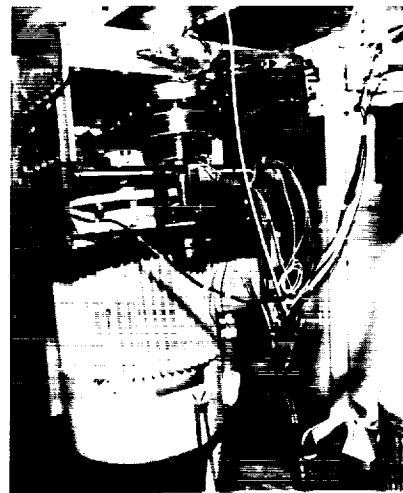


Figure 4. NASA LeRC MRTR drive assembly.

The number of data channels used was held to a minimum in keeping with the developmental purposes of this test vehicle. Torque changes were originally monitored by using a differential measuring device that recorded reaction torque changes from the drive system. This system proved to be unreliable and an in-line Lebow torquemeter was incorporated in the drive shaft for this test and other future work. A set of redundant speed pick-ups were located on the drive shaft because of the critical nature of this information. The vibration output was

recorded to detail the severity and timing of shedding events with respect to the torque data. Finally, the collective pitch angle was taken to document the rotor blade angles for the specific icing encounters.

All the instrumentation, except the second rotor rpm, was connected to a datalogger system that conditioned the information, converted it to engineering units, and downloaded it to a micro-computer (PC) for storage. The datalogger also provided updated information to a CRT screen for review by the model rotor operator. A variable data collection rate was incorporated in the software, but experience indicated a two second interval between data points provided adequate documentation. On occasion, data was taken at higher sampling rates to examine deicer pressurization effects on torque. The redundant speed set-up provided independent observation of rotor rpm in case the datalogger/pc system failed. This allowed a backup measure of minimum capability to control the rotor speed while the tunnel was being shutdown.

Small Tube Pneumatic De-Icing System

The BFGoodrich STP system is a variation of a conventional pneumatic deicer that uses low profile tubes (Figure 5 {CD-91-54270}) that are 1/4 and/or 3/8 inches (flat width). The tubes are inflated from an air connection that provides both inflation and deflation. The 125 psi supply air expands the elastomer tubes, which breaks the ice-to-surface bonds; the ice particles are then lifted from the airfoil by the airstream and carried away. During the non-activated periods the tubes have a vacuum applied to them to prevent the negative aerodynamic pressures from partially distending the tubes and disrupting the airflow. The diminished surface distortion with the small tube system creates a less severe aerodynamic performance penalty, and allows the removal of thinner ice layers than a conventional pneumatic deicer.

For the forced shedding segment of the test, the rotor blades had STP deicers that covered 6.98 cm (2.75 in) chordwise, 0.56 m (22.25 in) spanwise, and were 1.90 mm

(0.075 in) thick, (Figure 6 {C-92-4542}). The

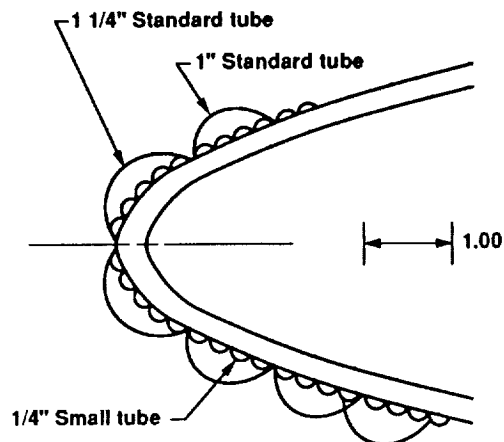


Figure 5. Schematic of BFGoodrich STP System.

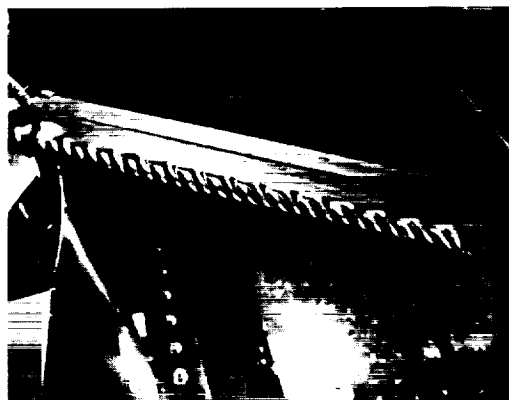


Figure 6. STP de-icers mounted on MRTR rotor blades.

deicers were wrapped symmetrically about the rotor blade leading edge, and the ends of the boots were tapered to blend into the outer skin of the airfoil on the upper and lower surfaces. The spanwise coverage started 2.22 cm (0.875 in) in from the blade tip. The inflation pressure was supplied by nitrogen (instead of air) to provide a moisture free pressure supply. The

N₂ was stored in a plenum with the output to the deicer regulated by an electrically operated flow valve. The nitrogen flowed through an air line and rotating pressure coupling in the mast above the rig to a "top hat" device that distributed the supply to two flexible lines connected to the STP deicers on each rotor blade (Figure 7 {C-92-4433}). The deicer actuation was controlled by a timer located in the IRT Control Room. Once the flow valve was actuated both deicer tubes inflated at the same time, with the pressure wave starting at the blade root of the airfoil and moving outward. It took approximately 1/4 second for the deicers to fully inflate.

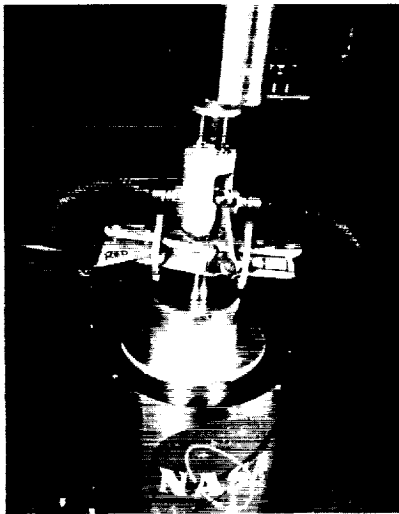


Figure 7. STP de-icer "top hat" assembly.

Impact Energy Measurement System (IEMS)

The IEMS is a combination of a sensor plate which can measure force-time traces due to an impact and imaging system which can be used to estimate the particle's size, velocity, and trajectory prior to impact. The energy absorbed by the sensor plate is derived by manipulation of the force-time trace recorded and estimation of the particle's incoming kinetic energy (see equation (6)). For this test, the sensing plate was mounted flush against the tunnel wall and had a total sensing area of 18" X 36". The plate consisted of 3 Force Sensing Resistors (FSR), each 18" X 12". A complete

description of the FSR's used is given below.

Two high-speed imaging devices were used to obtain the particle trajectory information. The two cameras were mounted in such a way as to have viewing planes orthogonal to each other. Thus, a complete 3-D trajectory of the particle could be obtained. In addition, the cameras also provided information about the particle velocity and size. Once the volume of the particle has been estimated based on the imaging information, the mass is calculated using an approximation for ice density. A complete description of the high speed cameras and their set-up in the IRT is given below.

Force Sensing Resistors (FSR)

FSR's are manufactured by Interlink Electronics. The sensor consists of two layers of film substrate, one of which supports interdigitating electrodes and the other supports a proprietary semiconductive polymer. The layers are laminated together with a combination adhesive/spacer material. The sensor maintains an open circuit until a force is applied to its surface. The resistance of the sensor changes with applied force. As force is applied anywhere on the sensing area, the resistance drops. This resistance drop is repeatable, and the sensor response to applied force can be calibrated for. A major advantage of using FSR's is that the resistance drop due to applied force is independent of impact location on the sensor. Thus, it is possible to obtain a large sensing area with few sensors. FSR's can operate in temperatures down to -30 °C. Moisture problems are limited to keeping the connection dry.

The challenge to applying this technology to measuring impact forces was in proper selection of an overlay material for the sensor and calibration. While FSR's are very durable, they cannot withstand the impact of an ice particle moving at several hundred feet per second without sustaining a significant amount of damage. Thus, a protective overlay had to be used. This overlay serves two purposes, the first of which is protection of the sensor. The overlay also serves to distribute the point load of the ice impact over a wider area of the

sensor. Many materials (including rubber and steel) of various thicknesses were tested. The material and thickness selected must provide a balance between protection and sensor sensitivity. The steel offered the greatest protection but reduced the sensor's sensitivity below an acceptable level. The rubber overlay allowed for the most sensitivity but changed the character of the impacts. It quickly became obvious that the selection of the overlay would dramatically affect the character of the force-time traces. A very spongy overlay (like rubber) produces force time traces which do not accurately model shed ice impacting on an aircraft component such as the fuselage. The material selected as an overlay was 0.032" thick 6061-T6 Aluminum. Given that aluminum is a very common aircraft material and it provided sensor protection without sacrificing too much sensitivity, it was chosen for the overlay material.

FSR's are fairly sensitive to the amount of area over which the force is applied. Thus, if the resistance of the sensor was measured when a 10 lb force was applied over a 1 in² area and then over a 5 in² area, they would be different. Therefore, all calibrations were performed using a point load force, to simulate an ice particle impact. The calibration procedure consisted of applying a known load to the FSR with the overlay attached and measuring the resistance of the sensor. The known load was provided by an impact hammer which was instrumented with a calibrated accelerometer. Since the mass of the hammer was known, the accelerometer output could be converted to a known force. A wide range of known forces were applied to the sensor. Afterwards, a plot of resistance vs. force could be made. Because resistance and force are related by a power law, a plot of $\ln(\text{Resistance})$ vs. $\ln(\text{Force})$ produces a straight line. Figure 8 shows a typical calibration plot for an FSR with the overlay applied. It can be seen that the data is indeed linear, with a slope of about -0.5. Therefore, the slope and intercept of the plot represent the calibration curve of the sensor. The slopes and intercepts for all the sensors calibrated were quite repeatable. The sensors were also calibrated at cold temperatures and it was found that

temperature only had a small effect on the calibration curves. Each of the three FSR's were incorporated into a voltage divider (Figure 9). The power supply provided a constant 8V. Thus, the voltage, V_o from each of the three FSR circuits was recorded during the impact event. The resistance (and hence, force) was calculated based on the recorded voltage data.

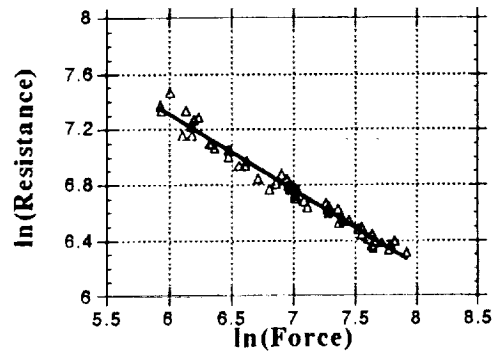


Figure 8. Typical calibration curve for FSR.

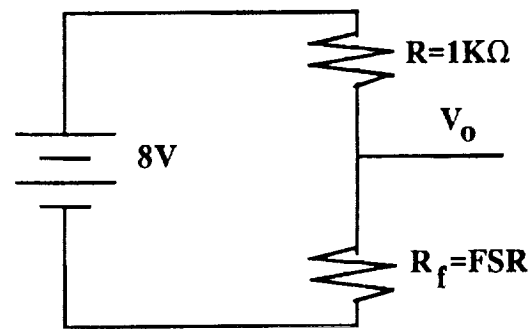


Figure 9. Voltage divider circuit for FSR.

The voltage data from each of the FSR's on the IEMS plate was recorded using a high speed data acquisition system. The sampling rate was 90,000 samples per second for each of the three channels used. This corresponds to a sample taken every 11 μsec. Given that a typical shed-ice impact event has a duration of 0.5 to 3 msec, it was felt that this sampling rate was adequate. For the shortest duration of 0.5 msec, this sampling rate still

provided about 45 data points in the curve, which was a sufficient number to integrate the curve accurately.

High Speed Imaging

The imaging part of the IEMS consisted of two high-speed imaging devices: a high-speed videography system and a high speed 16-mm motion picture camera. All the imaging data had an Inter Range Instrumentation Group (IRIG) time stamp recorded with the visual image. This feature provided a common standard to correlate all the different data collection processes to the same time reference. The data was then coupled with the shed-ice impact force-time trace to generate the impact energy of an ice particle strike.

The high speed videography system was a Kodak Ektapro 1000 motion analyzer. This system consists of an intensified imager, a controller, and the Ektapro 1000 processor. The imager has an image intensifier assembly which functions as an electronic shutter and light amplifier. This allows the imager to capture events in lower light and reduces the blurring of rapidly moving objects. The imager is connected to a controller which allows for adjusting the amount of time the electronic shutter is open (gating) during each frame. The imager sends a video output to the Ektapro processor where the event is stored on special cassette tapes. The event can be replayed instantly and viewed on a monitor. Depending on the field of view desired, the Ektapro can record images at a rate of up to 6000 frames per second. For this experiment, it was decided to use 1000 frames per second. This allowed for a large field of view.

The second camera in the system was a NAC model E-10/EE 16-mm high speed motion picture camera. This camera could run at speeds up to 10000 pictures per second (PPS). For the purposes of this test, it was decided to use 3000 PPS and either a 400 or 1200 foot film magazine. This combination yielded either 5 seconds, or 16 seconds of imaging data, respectively. The longer exposure time was used originally for the natural shedding events where there was much less control over the shedding environment.

During testing it became apparent that most of the data would be recorded during the forced shedding routines, so the 1200 foot film rolls were run for only a section of their total time to minimize film waste. The 16-mm high speed motion picture camera had provisions for a pulsed light emitting diode (LED) marking device on each side of the film sprocket drive to allow external information to be recorded on the edges of the film. An IRIG - B (microsecond) impulse signal was exposed onto the border of the film to provide time correlation to the Ektapro imaging data. On the opposite border, an event trigger mark was recorded which defined the start of the data acquisition system.

Two separate views were necessary to define the shed-ice particle information for the impact event (Figure 10). One view provided

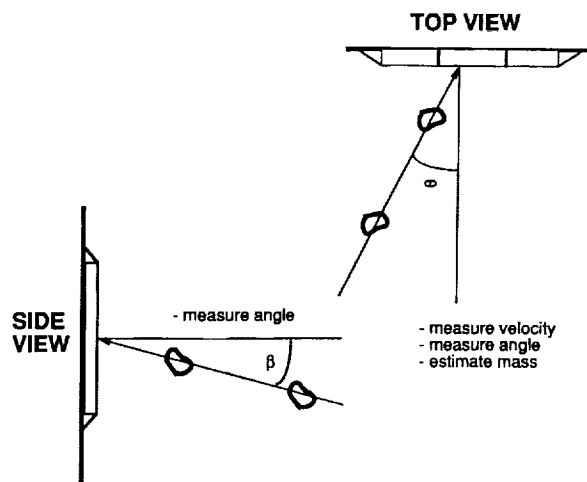


Figure 10. Views required to obtain 3-D trajectory of a shed ice particle.

the ice particle volume, velocity, and trajectory angle. This view was done with the high speed 16 mm film camera in an overhead shot. The camera was mounted vertically in the Control Room and viewed the ice impact area inside the test section through a window using two mirrors. The mirrors were first-surface, silver coated to minimize optical distortion, and provided maximum reflectivity. The other view provided the second trajectory angle needed. This was done with the Ektapro Intensified Imager in a side view perspective by

locating the camera in the IRT tunnel test section (Figure 11 [C-92-4312]). The camera was installed in a heated box near the tunnel wall upstream of the impact area.



Figure 11. View of Ektapro mounted inside tunnel.

TESTING PROCEDURE

Run Procedure

A typical test run for the MRTR consisted of setting the tunnel controls to the desired parameters, bringing the tail rotor speed up to a nominal operating rpm, and then starting up the tunnel. The overriding safety concern was the need to maintain the tail rotor tip speed considerably above the tunnel speed. If the tunnel speed were greater than the tip speed then large differences in lift between the advancing and trailing blades could occur which would cause instability in the teetering mechanism. Once the tunnel conditions were stable the tail rotor test operator set the rig rpm and collective pitch to the specified settings and started the pc data acquisition software. The imaging equipment and the IEMS system were set to standby, ready to record data during the actual shedding event. The tunnel operator then started the spray. Two different data acquisition scenarios were used depending on whether the ice shedding event was natural or forced.

The forced shed events were timed to build up differing amounts of ice to provide a range of ice particle impacts. The impact monitoring equipment was turned on just prior to the initiation of the deicer. The elapsed time from the start of the imaging equipment, the actuation and cycling of the deicer boots, and the ice expelling off the rotor blades was approximately 2 seconds.

The natural shedding scenario posed a much harder problem. The first attempt to capture information was based on building a historical database that would indicate when the ice would shed for repeat conditions. This proved impossible to do; the high sampling rates and camera speeds of the equipment constrained the data records to be less than 16 seconds in length, and the shed events were too random to be repeatable within that time window. A second approach was tried that worked on a limited basis. The torque level reached just prior to shedding was quite repeatable. As this level was approached the rig could be perturbed by momentarily increasing, then decreasing the speed. This action would usually initiate a shed event. Approximately 5-10 natural shed-ice impact events were recorded in this manner.

After the desired number of shed events, the IRT tunnel speed was brought to idle and the rig was shut down. After the run was over the researchers entered the test section to document post-test results. The assembly was then deiced and conditions set for the next run. If problems were encountered during the test run, the collective pitch and rig speed were decreased to nominal settings and then the tunnel rpm was returned to zero.

Post run information was gathered by taking 35 mm camera shots and visual observations. On a few occasions, heated aluminum blocks with a cutout contour of the airfoil profile were used to make a clean cut through the ice. A cardboard template was then held against the ice shape and a tracing made. Measurements of the ice thickness at various chord locations were taken and visual observations about the kind of ice and post-shed growth were recorded. The FSR's were examined for damage, the MRTR was deiced, and the imaging equipment was reloaded for

the next run.

Image Processing

The imaging data is currently being analyzed by two different processes. In the first, the Ektapro video tape images for a complete shed event are digitized inside the Ektapro processor and sent to an automated image processing software package on a workstation platform that determines the ice particle side view strike angle. In the second process, the film images are loaded on a data reduction platform that provides single frame viewing and digitization. Each picture frame for a shed event is digitized by a frame grabber in a PC. The images are then viewed consecutively, with an image processing package different than above, to get velocity and the top view strike angle. The ice particle area is generated by using a mouse to define the outer boundary. The number of pixels are counted within the bounded region and a scaling factor is applied to this value to convert to engineering units. Ice particle thickness can be found in a similar manner.

In order to determine the particle size and velocity the correct scale factor must be known. Before the test began, the high speed motion picture camera was mounted in the exact location it would be in for the test and images of a grid scale with 1-inch squares were recorded. This provided a reference length for the image. The grid scale was placed perpendicular to the sensor plate on the test section wall. The grid shots were then taken on 16-mm film by the high speed motion picture camera at the midpoint of the sensor and ± 6 in. vertically. Thus, a total of 3 scale factors were determined. The Ektapro view determined which scale factor to be used by showing vertically where the particle struck the sensor. A density will be applied to the ice particle to calculate the mass. The density of the ice is estimated based on the average temperature for the leading edge of the rotor blade during the test run.

RESULTS

As stated in an earlier section, over 300 shed-

ice impact events were recorded throughout the 16 days of testing. The imaging data from each of these events is currently being reduced, thus a detailed discussion of the results is not possible at this time. This section will concentrate on presenting a few samples and discussion of the force-time traces recorded.

Initially, it was hoped to test over a very wide range of rotor tip speed. This would translate into a wide range of incoming particle velocity and hence, kinetic energy. Due to vibration problems with the MRTR, the tip speed was restricted to relatively low levels (no higher than 560 ft/sec and most of the data between 450 and 500 ft/sec). Despite this, a wide range of peak impact forces were recorded (ranging from 0.5 to 200 lbf peak force).

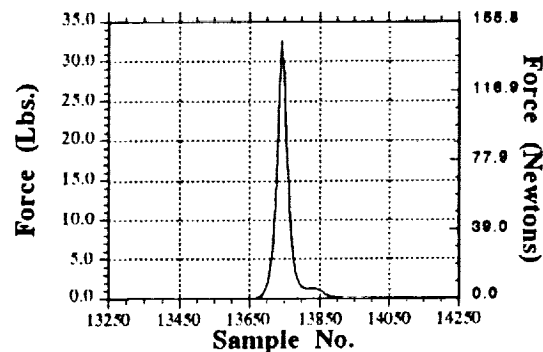


Figure 12. Typical force-time trace of a shed ice particle impact.

Figure 12 shows an example of a typical force-time trace taken during the experiment. For this case, the peak force is about 32 lbf. This corresponds to a significant local stress on the plate because the force is applied essentially as a point load. The overall duration of the impact event can be seen to be approximately 250 samples. As noted earlier, the sampling rate was 90,000 samples per second. Thus, the impact duration for this case is about 2.8 msec. For the data analyzed to date, the impact duration ranged from 0.5 msec to 3 msec. An example of a very low impact force (peak force 0.5 lbs) trace is shown in Figure 13 and a very high impact

force (peak force 190 lbs) case is shown in Figure 14. The impact duration is smaller

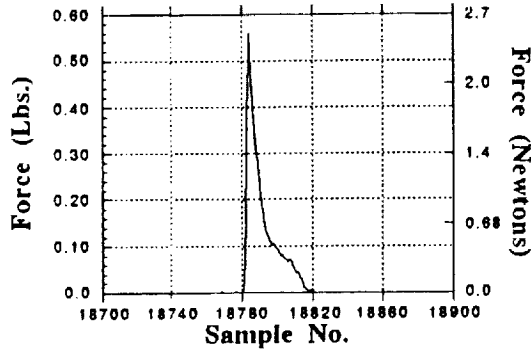


Figure 13. Force-time trace of a low force ice particle impact.

for the low force case (about 0.5 msec). Although not all of the data has been analyzed, the trend appears to be smaller impact durations for lower impact force cases. It is also interesting to note the shape of the curve

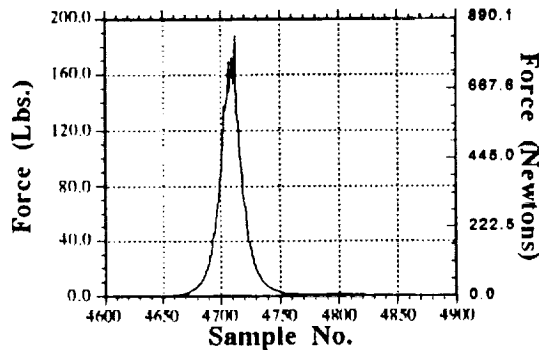


Figure 14. Force-time trace of a high force ice particle impact.

for the high-force case. Three peaks can be seen which seems to indicate that the ice particle broke up into several smaller pieces upon its initial impact. This is not too surprising given that the particle that would produce a peak impact force of 190 lbf at the velocities discussed earlier would have to be very large, relatively speaking.

When the de-icer was operated, many

particles were shed from the rotor blades. Often, several particles would strike the IEMS sensor at virtually the same time. Figure 15 shows a typical example of a multiple particle impact trace. A total of three impact events

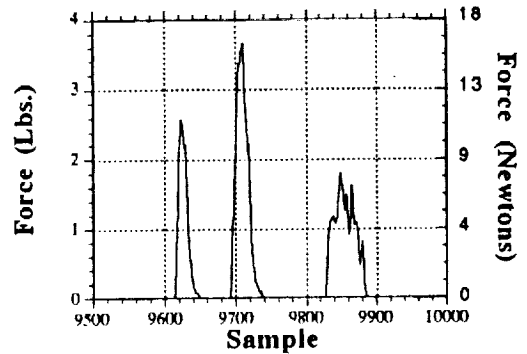


Figure 15. Force-time trace of multiple ice particle impact.

were captured. The first two traces are "clean", while the third trace is jagged. The third trace indicates that several particles struck at almost exactly the same time. This presents a problem in obtaining the impact energy associated with this strike. As indicated in an earlier section, the analysis procedure includes the integration of the force-time trace associated with a single particle. Thus the traces which are "polluted" with other particle impacts are unusable for this analysis; while the first two traces in Figure 15 will be used in the analysis, the third trace will not. Of the 300 impact events recorded, only about 70 impacts were single particle impacts which could be integrated to find the impact energy.

SUMMARY AND CONCLUSIONS

The NASA LeRC Model Rotor Test Rig has been tested in the Icing Research Tunnel in order to study impact forces associated with shed ice particles. An Impact Energy Measurement System consisting of Force Sensing Resistors and high-speed imaging devices has been developed. During the 16 days of actual testing, over 300 impact events were recorded on the IEMS. Of these,

about 70 have been determined to be useful for calculation of the impact energy associated with the impact event. The imaging data which is required to obtain particle size, velocity, and trajectory is currently being reduced. Ongoing tests of the IEMS are being performed at the University of Toledo ice gun facility to provide a validation data base for comparison to the data taken in the IRT.

The successful testing of the IEMS in the IRT has demonstrated that impact forces associated with shed-ice particles can be measured. Data gathered in this test appear to be reasonable. A more detailed evaluation of the method will be performed once all of the imaging data has been reduced and comparisons made to the data taken at the University of Toledo.

ACKNOWLEDGEMENT

The authors of this paper would like to sincerely thank Erwin Meyn for his invaluable technical assistance in the development of the IEMS.

REFERENCES

¹ Britton, R.K., "Development of an Analytical Method to Predict Helicopter Main Rotor Performance in icing Conditions," AIAA Paper 92-0418, January 1992 (Also, NASA CR-189110, 1992).

² Henderson, G.R. and Server, W.L., "An Optical System for Measurement of Energy for Pendulum Impact Machines," *Instrument Society of America Transactions*, Vol. 18, No. 3, 1979, pp 35-39.

REPORT DOCUMENTATION PAGE			Form Approved OMB No. 0704-0188	
Public reporting burden for this collection of information is estimated to average 1 hour per response, including the time for reviewing instructions, searching existing data sources, gathering and maintaining the data needed, and completing and reviewing the collection of information. Send comments regarding this burden estimate or any other aspect of this collection of information, including suggestions for reducing this burden, to Washington Headquarters Services, Directorate for Information Operations and Reports, 1215 Jefferson Davis Highway, Suite 1204, Arlington, VA 22202-4302, and to the Office of Management and Budget, Paperwork Reduction Project (0704-0188), Washington, DC 20503.				
1. AGENCY USE ONLY (Leave blank)		2. REPORT DATE January 1993		3. REPORT TYPE AND DATES COVERED Technical Memorandum
4. TITLE AND SUBTITLE An Overview of Shed Ice Impact Studies in the NASA Lewis Icing Research Tunnel			5. FUNDING NUMBERS WU-505-68-11	
6. AUTHOR(S) Randall K. Britton and Thomas H. Bond				
7. PERFORMING ORGANIZATION NAME(S) AND ADDRESS(ES) National Aeronautics and Space Administration Lewis Research Center Cleveland, Ohio 44135-3191			8. PERFORMING ORGANIZATION REPORT NUMBER E-7492	
9. SPONSORING/MONITORING AGENCY NAMES(S) AND ADDRESS(ES) National Aeronautics and Space Administration Washington, D.C. 20546-0001			10. SPONSORING/MONITORING AGENCY REPORT NUMBER NASA TM-105969 AIAA-93-0301	
11. SUPPLEMENTARY NOTES Prepared for the 31st Aerospace Sciences Meeting sponsored by the American Institute of Aeronautics and Astronautics, Reno, Nevada, January 11-14, 1993. Randall K. Britton, Sverdrup Technology, Inc., NASA Lewis Research Center Group, 2001 Aerospace Parkway, Brook Park, Ohio 44142 and Thomas H. Bond, NASA Lewis Research Center. Responsible person, Randall K. Britton, (216) 891-2237.				
12a. DISTRIBUTION/AVAILABILITY STATEMENT Unclassified - Unlimited Subject Category 02			12b. DISTRIBUTION CODE	
13. ABSTRACT (Maximum 200 words) One of the areas of active research in commercial and military rotorcraft is directed toward developing the capability of sustained flight in icing conditions. The emphasis to date has been on the accretion and subsequent shedding of ice in an icing environment, where the shedding may be natural or induced. Historically, shed-ice particles have been a problem for aircraft, particularly rotorcraft. Because of the high particle velocities involved, damage to a fuselage of other airframe component from a shed-ice impact can be significant. Design rules for damage tolerance from shed-ice impact are not well developed because of a lack of experimental data. Thus, the NASA Lewis Research Center (LeRC) has begun an effort to develop a database of impact force and energy resulting from shed ice. This effort consisted of a test of NASA LeRC's Model Rotor Test Rig (MRTR) in the Icing Research Tunnel (IRT). Both natural shedding and forced shedding were investigated. Forced shedding was achieved by fitting the rotor blades with achieved by fitting the rotor blades with Small Tube Pneumatic (STP) deicer boots manufactured by BF Goodrich. A detailed description of the test is given as well as the design of a new impact sensor which measures the force-time history of an impacting ice fragment. A brief discussion of the procedure to infer impact energy from a force-time trace are required for the impact-energy calculations. Recommendations and future plans for this research area are also provided.				
14. SUBJECT TERMS Shed ice impact; Measurement; Icing			15. NUMBER OF PAGES 14	
			16. PRICE CODE A03	
17. SECURITY CLASSIFICATION OF REPORT Unclassified	18. SECURITY CLASSIFICATION OF THIS PAGE Unclassified	19. SECURITY CLASSIFICATION OF ABSTRACT Unclassified	20. LIMITATION OF ABSTRACT	

